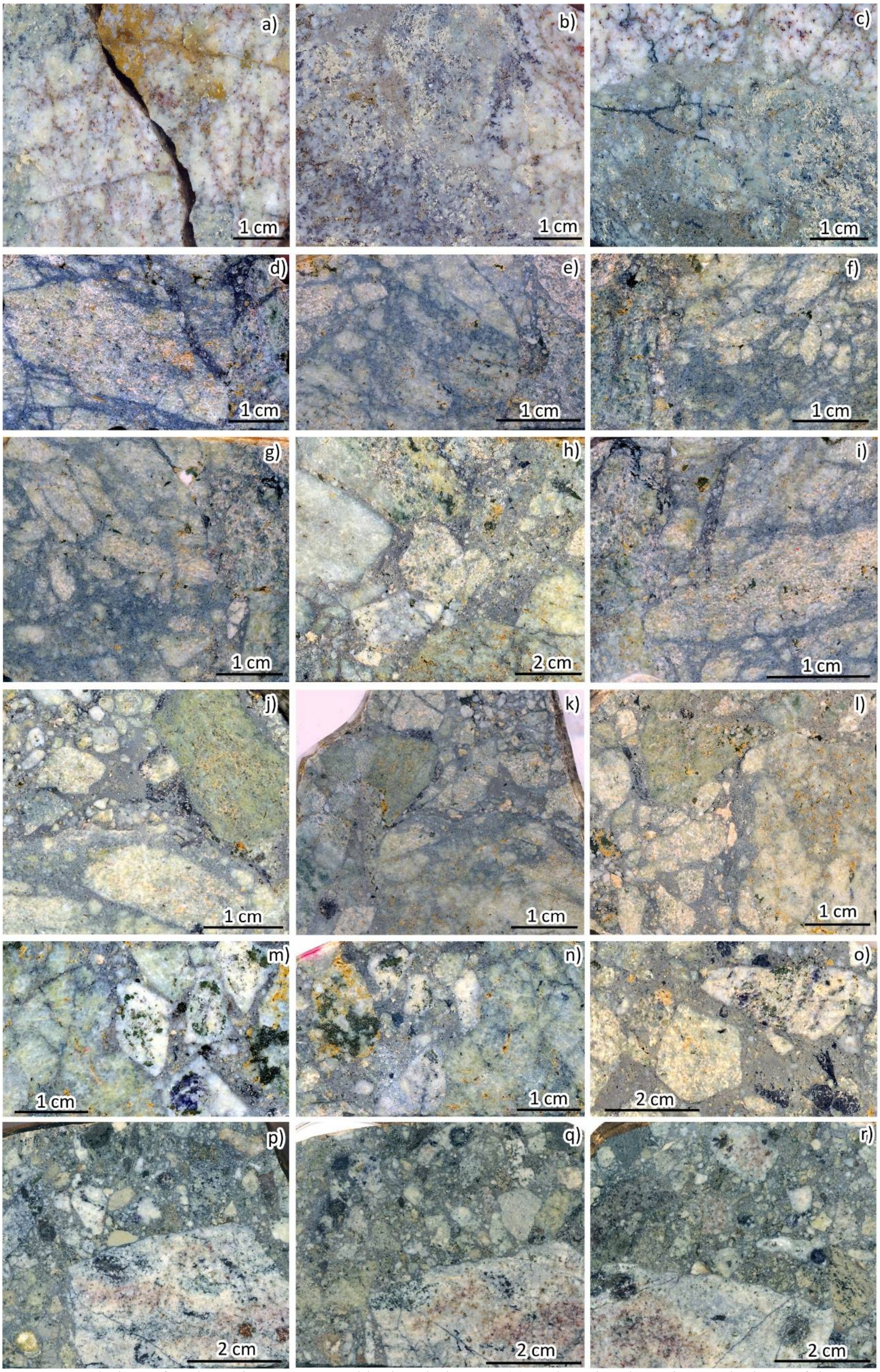

Fig. S1-1. General view of rock sections penetrated by borehole G-2: (a) – altered carbonatites at the base of the penetrated section (int. 259-260 m; T-197-23); (b, c) – calcite carbonatites partially replaced by secondary minerals (int. 258-259 m; T-198-23); (d-p) – textures of carbonatite breccias (int. 217.2-217.5 m; T-205-23); (q, r) – different surfaces of carbonatite breccia sections with concentrically zoned spherical formations composed of fluorite and sulfides, with int. 217.0-216.5 m; T-206-23.

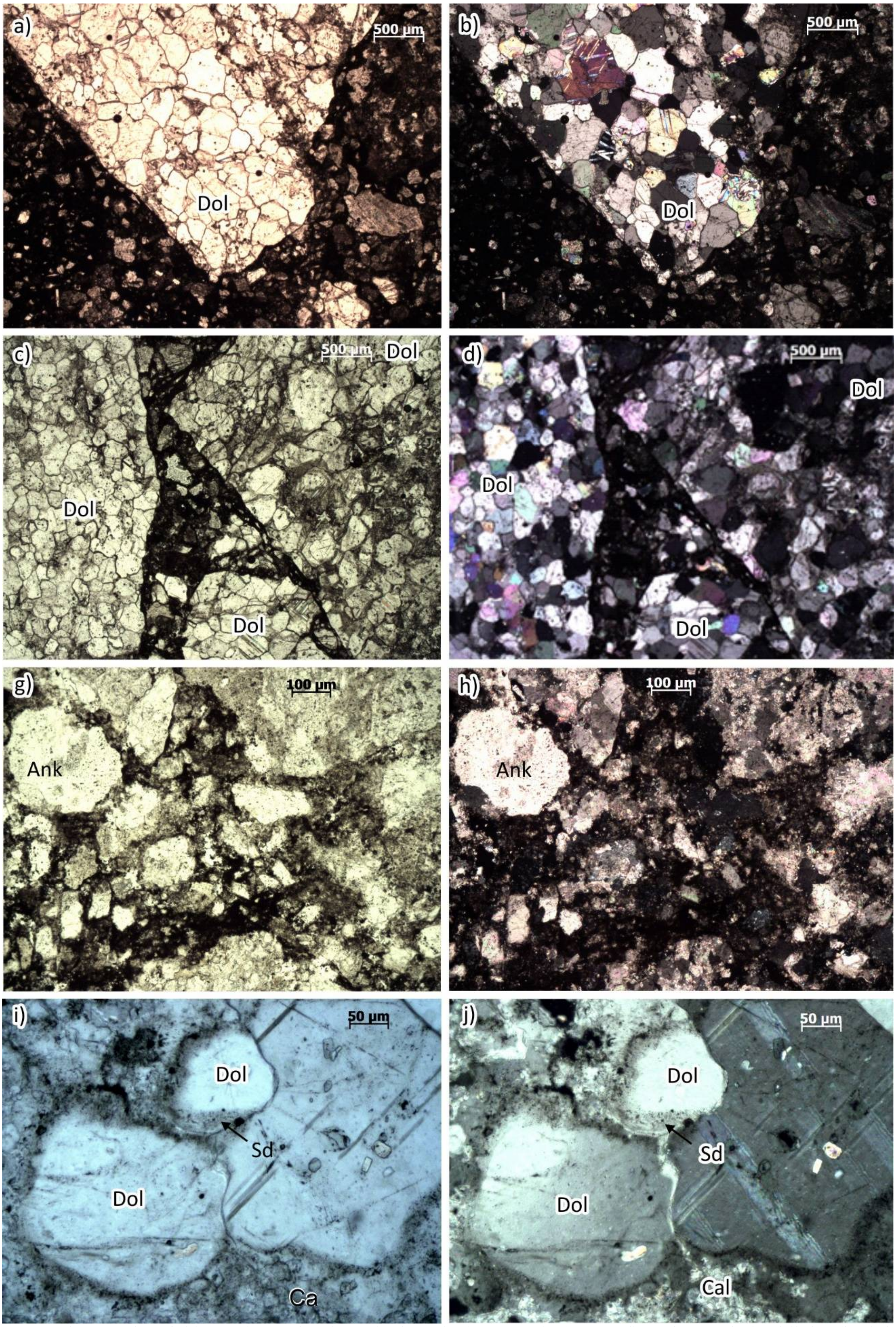

Fig. S1-2. Micrographs of thin sections of carbonatite breccia (T-205-23): (a, c, g, i) – plane polarized light; (b, d, h, j) – crossed nicols; (a, b, c, d) – large angular fragments of dolomite carbonatite with mosaic polygonal structure among fine-grained matrix represented by carbonates and cryptogranular brown cement; (g, h) – rounded fragments of ankerite carbonatites among carbonate matrix and cryptogranular brown cement; (i, j) – rounded fragments of dolomite carbonatite are replaced by siderite on the surface, calcite in the interfragmental space. Mineral designations: Dol – dolomite; Sd – siderite; Cal – calcite.

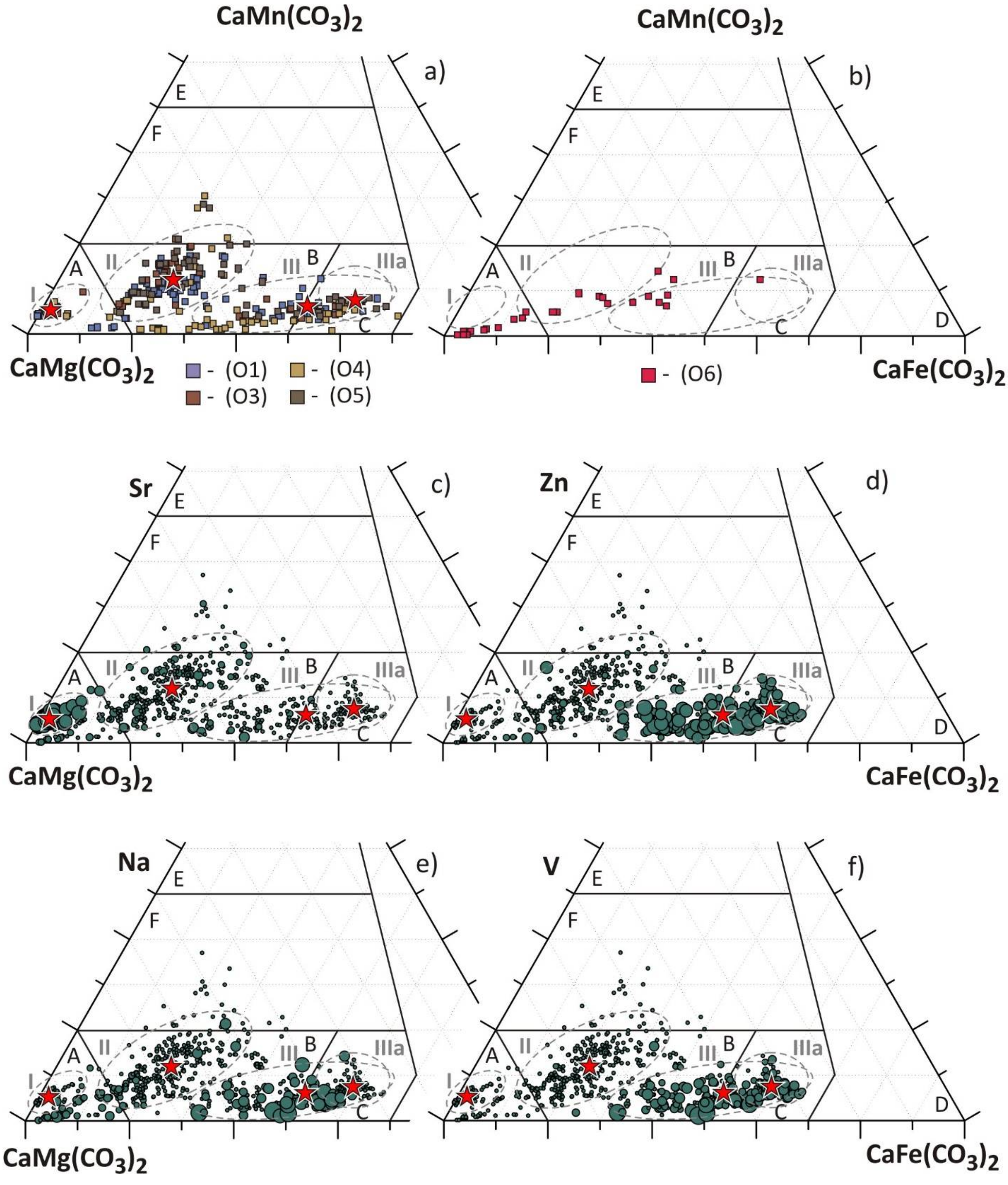

Fig. S1-3. Composition of double carbonates from various breccia fragments of well G2 (a, b), and relative contents of trace elements Sr and Na (c, d), and elements consistently determined in carbonate analysis – Na and V (e, f): (A: Dolomite with $CaMg(CO_3)_2 > 0.8$) B+C: ankerite [Chang, 1996]. C: ankerite proper. D: solubility limit field of $CaFe(CO_3)_2$ in ankerite [Essene, 1983]. E+F: kutnogorite according to [Chang, 1996].

The bable size indicates the relative abundance of elements (c-f). The red star is the average for samples I, II, III, and IIIa (Table 1). O1-6 are the fragment numbers.

Table S1-1. **Concentration rangesofelements and relative errors inwhole-rock XRF analysis.**

Component	Measured range, wt.%	Relative error*,%
Na_2O	0.04-15	28-3.5
MgO	0.05-45	30-1.7
Al_2O_3	0.01-100	30-1.1
SiO_2	0.01-100	30-0.7
P_2O_5	0.01-2	21-4.3
K_2O	0.01-10	30-3.5
CaO	0.01-100	30-1.2
TiO_2	0.01-100	27-0.8
MnO	0.01-2	24-3.4
Fe_2O_3	0.01-100	30-0.7
BaO	0.005-0.5	30-16
SO_3	0.04-60	21-1
V_2O_5	0.01-0.15	25-16
Cr_2O_3	0.01-50	14-2.5
NiO	0.01-0.3	23-5
LOI	0.2-50	11-1.4

Note: LOI – loss on ignition, * - for lowerand upper concentration bounds.

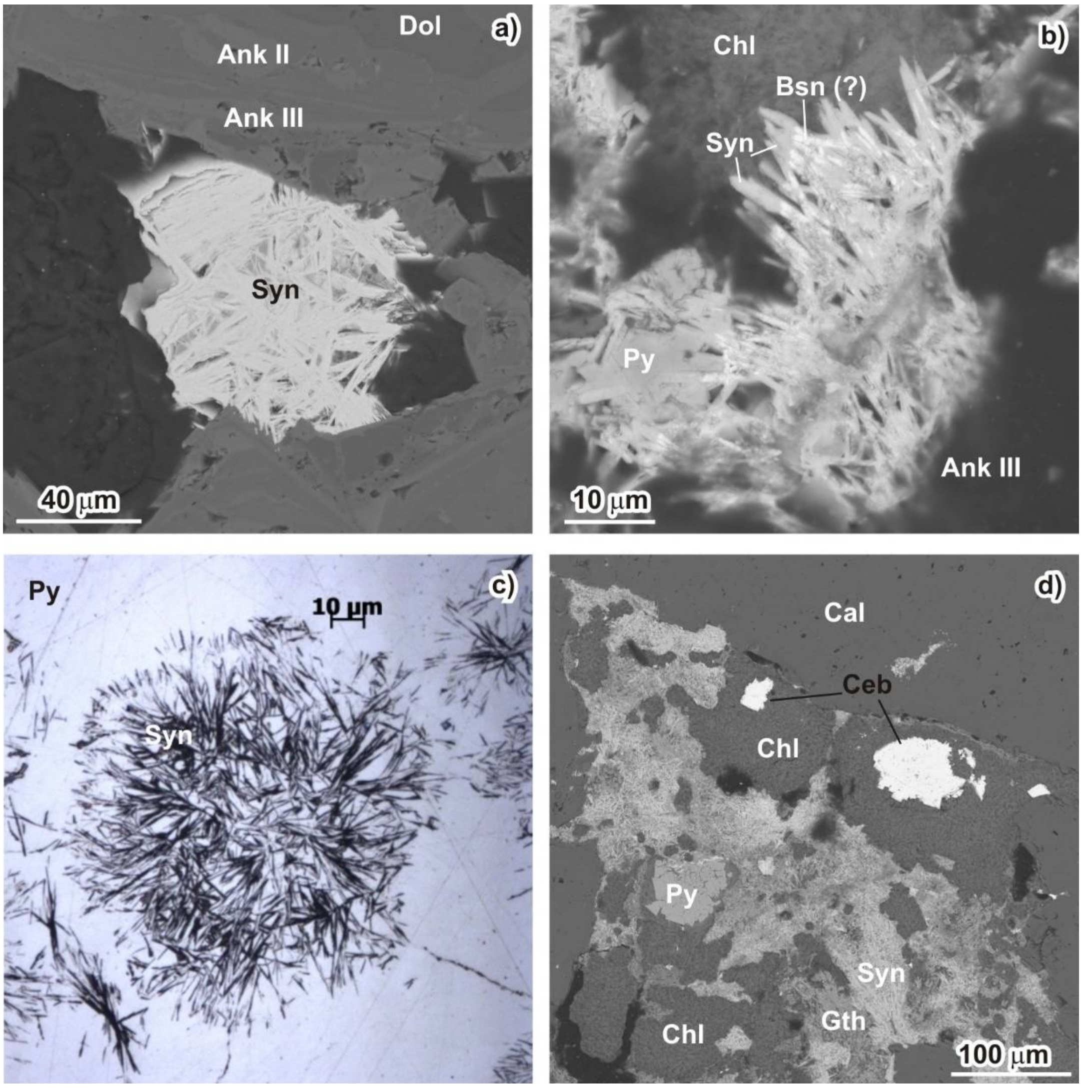

Fig. S1-4. F-REE-carbonates from breccia fragments of well G2: (a) – synchysite-(Ce) aggregate in the cavity of dolomite carbonatite weakly replaced by ankerite (O1); (b) synchysite-(Ce) and parisite-(Ce) or bastnaesite-(Ce) aggregate in association with pyrite and chlorite in the cavity of dolomite carbonatite weakly replaced by ankerite (O1); (c) synchysite-(Ce) spherulite in pyrite; (d) synchysite-(Ce) and zebaite-(Ce) aggregates in association with Fe-chlorite and pyrite. Mineral designations: Dol - dolomite, Ank II and III - ankerite of compositions corresponding to regions II and III (see Fig. 6), Cal - calcite, Chl - chlorite, Py - pyrite, Syn - synchysite-(Ce), Bsn - bastnaesite-(Ce), Ceb - zebaite-(Ce), Gth - goethite.

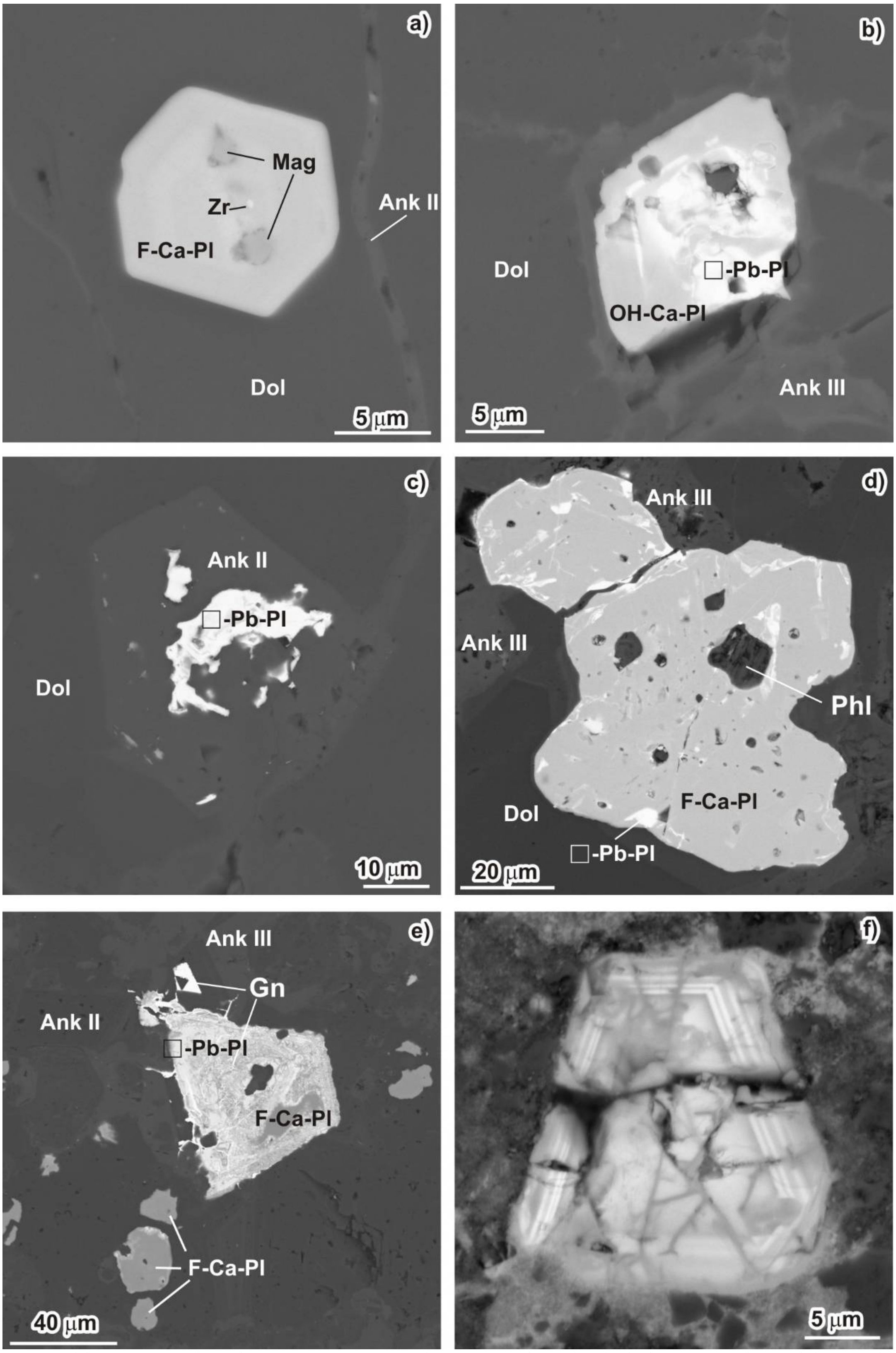

Fig. S1-5. Pyrochlore group minerals from fragments and cement of breccias in hole G2: (a) fluorcalciopyrochlore with inclusions of magnetite and Zr mineral (zircon?) from dolomite carbonatite weakly replaced by ankerite (O1); (b) hydroxylcalciopyrochlore from dolomite carbonatite weakly replaced by ankerite (O1); (c) ankerite II pseudomorph after pyrochlore crystal with preserved kenoplumbopyrochlore fragments from dolomite carbonatite weakly replaced by ankerite (O1); (d) fluorcalciopyrochlore from dolomite carbonatite weakly replaced by ankerite (O2); (d) fluorcalciopyrochlore and kenoplumbopyrochlore in association with galena from dolomitic carbonatite weakly replaced by ankerite (O2); (e) hydrocalciopyrochlore with significant Sr, Ba and Pb content in the A position, from the breccia cement. Mineral designations: Dol - dolomite, Ank II and III - ankerite of compositions corresponding to regions II and III (see Fig. 6), Mag - magnetite, Gn - galena.

Table S1-2. **Major oxides (wt.%) and element abundances (ppm) in carbonatite breccias exposed by hole G2**

Component	Method of analysis	T-208-23	T-211-23	T-205-23	T-206-23	T-212-23	T-207-23	T-210-23	T-199-23	T-203-23	T-198-23	T-196-23
Interval, m		210	211	216.5-217	217-217.5	218.5	230	231	242.5	255	258.5	277
SiO_2	XRF	4.31	15.41	2.49	4.65	4.12	0.40	4.86	0.89	1.45	1.42	7.52
TiO_2	XRF	1.51	2.53	0.92	0.96	1.31	0.09	1.62	0.37	0.51	1.44	1.97
Al_2O_3	XRF	0.03	3.90	0.32	0.40	0.75	<	0.19	0.14	0.09	0.67	1.88
Fe_2O_3	XRF	9.32	12.64	7.35	6.34	9.03	2.57	37.47	3.42	5.70	8.40	10.6
MnO	XRF	0.72	0.54	2.55	1.40	1.26	0.92	1.55	0.61	1.50	1.94	0.62
MgO	XRF	0.12	0.82	12.23	4.89	0.86	1.67	0.06	0.54	3.99	9.72	0.81
CaO	XRF	45.0	32.0	31.9	40.5	44.8	51.5	25.6	52.1	44.0	31.1	41.5
Na_2O	XRF	0.07	<	<	<	<	<	<	<	<	<	<
K_2O	XRF	0.04	2.69	0.16	0.10	0.24	<	<	<	0.10	0.06	0.14
P_2O_5	XRF	6.10	2.94	3.64	2.72	5.35	2.36	6.69	3.96	3.35	0.87	3.74
SO_3	XRF	0.49	1.54	0.37	1.29	1.65	1.56	0.24	0.25	1.72	1.46	1.17
Nb_2O_5	XRF	0.77	0.81	0.39	1.26	0.64	0.25	0.37	0.21	0.97	4.79	0.63
LOI	XRF	28.7	22.5	36.2	33.9	28.3	37.8	17.5	35.8	35.5	36.2	27.4
Σ	XRF	97.5	98.7	98.8	98.6	98.6	99.2	96.6	98.4	99.2	98.5	98.2
Li	ICP-AES	7.2	38	29	16	47	2.5	11	4.8	4.7	15	13
Be	ICP-AES	37	40	11	16	25	3.7	68	8.0	5.8	15	31
Sc	ICP-MS	193	124	102	94	96	33	115	59	55	91	119
V	ICP-AES	600	1300	580	480	920	88	1500	310	260	530	800
Cr	ICP-AES	9.2	160	10	12	75	15	54	7.1	4.9	10	36
Co	ICP-AES	4.9	14	4.4	7.5	12	7.6	33	3.4	5.7	11	13
Ni	ICP-AES	15	58	5.5	8.9	27	5.3	85	6.0	3.4	5.9	30
Cu	ICP-AES	4.6	11	2.0	8.0	2.2	2.2	24	<1	4.3	12	5.6
Zn	ICP-AES	1900	1700	2100	1700	1600	500	2500	580	2600	3900	2100
Ga	SR-XRF	23.4	10	17.1	29.6	10	10.3	<1	9.5	11.7		34.2
As	ICP-AES	100	80	54	99	77	58	250	110	37	78	130
Rb	ICP-MS	3.2	20.4	6.3	3.0	7.1	<3	<3	74.2	2.3	6.8	7.0
Sr	ICP-MS	4872	3089	4119	3254	4917	2452	5635	3395	2919	2248	3347
Y	ICP-MS	2882	883	712	760	1153	553	1570	982	565	373	1323
Zr	ICP-MS	346	198	130	416	205	92	104	153	350	2121	186
Nb	ICP-MS	5418	5316	2423	9109	4380	1944	2089	1469	6283	30761	3802
Mo	ICP-AES	2.8	3.5	<0.5	18	3.4	3.4	35	2.8	7.0	23	3.5
Cd	ICP-AES	2.7	2.9	3.5	2.5	2.7	2.0	1.2	4.6	16	30	4
Sn	ICP-AES	<5.0	5.8	<5.0	<5.0	6.3	<5.0	<5.0	<5.0	<5.0	<5.0	<5.0
Cs	ICP-MS	<1	<1	1.1	<1	<1	<1	<1	<1	<1	<1	<1
Ba	ICP-MS	1488	1697	1722	1603	1356	497	3409	602	457	1132	1573
La	ICP-MS	2785	2291	1375	2407	1973	1471	6272	2802	1055	2162	3348
Ce	ICP-MS	5124	3773	2429	4226	3391	2474	10272	4586	2005	4248	5360
Pr	ICP-MS	480	366	225	397	322	240	973	433	188	398	523
Nd	ICP-MS	1684	1251	786	1373	1137	806	3320	1429	651	1367	1755
Sm	ICP-MS	314	199	148	216	190	112	466	194	108	168	304
Eu	ICP-MS	137	75	60	83	77	39	156	66	40	49	122
Gd	ICP-MS	469	231	192	254	252	128	498	218	125	153	409
Tb	ICP-MS	82	38	31	37	44	21	71	32	19	18	60
Dy	ICP-MS	443	179	148	167	232	104	323	171	98	75	271
Ho	ICP-MS	91	31	27	28	41	18	53	33	18	14	45
Er	ICP-MS	231	73	71	69	94	44	138	78	45	30	101
Tm	ICP-MS	32	10	7	8	11	5	17	10	6	4	12
Yb	ICP-MS	178	56	37	42	62	29	92	59	36	22	70
Lu	ICP-MS	23	7	4	4	7	3	12	8	5	3	9
Hf	ICP-MS	9.9	4.4	3.6	10.3	4.7	2.8	3.1	4.3	7.7	33.9	5.3
Ta	ICP-MS	8.3	6.7	15.2	15.9	11.0	1.6	1.8	6.9	3.0	5.6	6.2
Pb	ICP-MS	411	279	343	385	436	128	222	118	95	493	333
Th	ICP-MS	542	203	160	263	555	150	720	247	104	200	370
U	ICP-MS	2.0	1.6	2.7	5.8	1.5	3.2	3.5	2.2	4.3	10.8	2.2
Ln+Y, %	ICP-MS	1.50	0.95	0.63	1.01	0.9	0.6	2.42	1.11	0.50	0.91	1.37
Th/U	ICP-MS	270	125	60	46	366	47	207	111	24	18	166

Note: LOI – loss on ignition,< – below detection limit.

Table S1-3. **Major oxides (wt.%) in in fragments and cement of breccia samples T-205-23 (217.5-217 м) and T-206-23 (217-216.5 м)**

Polished section	PS.205-1a		PS.205-1б						PS.206-3б
Fragment #	(O1) (Fig. 6a) №№10 и14 (Fig. 3)		(O3) (Fig. 6d) ≈№17 (Fig.3)		(O4) (Fig. 7a)		(O2) (Fig. 6c)	(O5) (Fig. 7c)	(O6) 1-5 (Fig. 7d)
Material	Fragment	Cement	(O3-1)	(O3-2)	Fragment	Cement	Cement	Fragment	Fragment
SiO_2	0.71	2.87	1.46	0.28	3.96	13.23	4.97	1.10	1.28
TiO_2	<	0.82	0.39	0.31	0.09	1.84	1.46	0.09	0.14
Al_2O_3	0.17	0.89	0.34	0.09	0.45	4.08	1.47	<	0.42
FeO	2.44	4.88	6.80	4.11	7.41	5.29	8.30	8.50	4.40
MnO	2.07	1.34	2.70	2.24	1.80	1.42	1.80	5.28	0.66
MgO	17.9	4.51	15.29	4.95	14.94	3.66	5.22	12.11	2.31
CaO	27.8	29.83	29.06	41.18	26.41	29.92	29.01	29.09	46.58
Na_2O	<	<	<	<	0.25	<	<	<	<
K_2O	0.12	0.58	0.30	0.05	0.62	2.95	1.00	0.04	0.04
BaO	<	<	<	<	<	<	<	<	0.15
SrO	0.85	0.6	0.51	<	0.71	0.61	0.50	0.25	0.27
ZnO	<	<	0.13	0.33	0.41	0.20	0.33	<	0.21
V_2O_3	0.04	<	0.11	<	0.11	<	0.21	<	<
REE_2O_3	<	0.68	0.38	0.17	<	1.07	1.58	<	0.34
Nb_2O_5	<	0.41	<	<	0.96	0.95	0.91	<	0.58
P_2O_5	<	6.62	0.35	0.44	<	5.79	5.92	0.18	1.53
SO_3	<	0.55	<	0.09	<	<	1.80	<	0.18
F	<	<	<	1.70	0.48	<	<	<	<
Σ	52.3	54.58	57.98	56.59	58.56	71.20	64.41	56.62	59.81

Note: < – below detection limit.

Table S1-4. **Major oxides (wt.%) (mean (median)/minimum-maximum) in carbonatites and host carbonate deposits [Ponomarchuk et al., 2024]**

Component	Phosphorus-rare metal (polymineral) carbonatites		Rare metal (ankerite) carbonatites	Ulakhan-Kurungskaya (R_1*uk*) formation
	Hole 6151, n=5	Hole 4041, n=11	Hole 4849, n=15	n=1
SiO_2	5.6 (5.4) 3.8-7	2.6 (2.6) 0.55-3.9	2.21 (2.2) 1.05-4.6	3.57
TiO_2	0.3 (0.16) 0.04-1.02	0.27 (0.2) 0.15-0.46	1.06 (0.79) 0.36-3.85	0.04
Al_2O_3	0.16 (0.1) 0.1-0.4	0.39 (0.3) 0.1-1.5	0.16 (0.1) 0.1-0.54	1.5
Fe_2O_3	7.61 (7.64) 6.02-8.7	1.09 (0.84) 0.37-2.1	1.85 (1.55) 0.1-3.66	0.14
FeO	2.16 (3.37) 1.65-2.52	3.44 (2.87) 2.3-6.75	11.04 (9.09) 6.8-19.98	nd
MnO	0.7 (0.68) 0.54-0.88	1.44 (1.43) 1.14-1.81	4.95 (5.53) 2.81-7.45	0.01
MgO	0.75 (0.75) 0.5-1	2.85 (2.57) 2-4.37	7.57 (7.12) 5.12-12.25	20.5
CaO	42.3 (41.75) 41-45.25	45.4 (46.5) 38.8-48.75	29.98 (29.75) 18.15-37.5	27.2
Na_2O	0.12 (0.12) 0.12-0.12	0.1 (0.1) 0.08-0.12	0.08 (0.08) 0.05-0.11	<0.1
K_2O	0.28 (0.12) 0.11-0.91	0.46 (0.5) 0.05-0.84	0.18 (0.08) 0.05-0.92	0.1
CO_2	31.6 (31.5) 29.74-34.32	36.4 (36.2) 35.1-38.43	29.6 (28.1) 25.34-37.0	nd
P_2O_5	3.97 (3.3) 3.16-5.28	3.82 (3.95) 2.3-4.95	1.02 (0.99) 0.31-1.61	0.11
SO_3	0.38 (0.39) 0.25-0.54	1.31 (1.15) 0.69-2.33	2.54 (1.69) 0.75-5.09	0.04
LOI	0.94 (0.83) 0.65-1.6	nd	nd	46.8
Σ	96.9 (96.7) 95.5-97.9	99.5 (99.7) 98.2-100.73	92.35 (92.16) 88.51-98.8	99.94
Ln+Y, %	0.59 0.57-0.6 (n=2)	0.39 (0.37) 0.32-0.51 (n=4)	1.28 (1.37) 0.64 – 1.65 (n=9)	0.014

Note: LOI – loss on ignition, n – number of analyses, nd – no data

Table S1-5. **Isotopic compositions ($\delta^{13}C$ ‰, $\delta^{18}O$ ‰) of various breccia fragments and cement (samples T-205-23 and T-206-23)**

No	Sample	Description, (fragment designation)	$\delta^{13}C_{SMOW}$‰	$\delta^{18}O_{PDB}$‰
1	T-206-23-1	Large fragments, composed mainly of calcite, contain visible concretions of fluorite, (O6)	-3.1±0.1	17.6±0.5
2	T-206-23-1	Cement	-3.1±0.1	16.6±0.5
3	T-206-23-1	Small greenish fragments	-2.8±0.1	18.0±0.1
4	T-206-23-1	Cement	-2.9±0.1	17.1±0.3
5	T-206-23-1	Large fragments, composed mainly of calcite, contain visible concretions of fluorite, (O6)	-2.6±0.1	17.1±0.2
6	T-206-23-1	Large fragments, composed mainly of calcite, contain visible concretions of fluorite, ≈ (O6)	-3.2±0.1	17.7±0.2
7	T-205-23-1	Fragments of greenish carbonatite	-3.1±0.04	16.3±0.4
8	T-205-23-1	Fragments of greenish carbonatite	-2.9±0.1	17.3±0.2
9	T-205-23-1	Cement	-3.0±0.3	16.9±0.1
10	T-205-23-1	Fragments of dolomitic carbonatite, (O1)	-4.4±0.1	10.8±0.6
11	T-205-23-2	Fragments of greenish carbonatite	-3.2±0.2	15.6±0.1
12	T-205-23-2	Cement	-3.2±0.1	14.8±0.1
13	T-205-23-2	Fragments of greenish carbonatite	-3.4±0.1	14.8±0.1
14	T-205-23-2	Fragments of dolomitic carbonatite, ≈ (O1)	-4.2±0.03	11.3±0.3
15	T-205-23-2	Large fragments, composed mainly of calcite, contain visible concretions of fluorite, ≈ (O6)	-2.8±0.04	17.9±0.2
16	T-205-23-2	Fragments of variegated carbonatite	-3.5±0.1	14.2±0.3
17	T-205-23-3	Fragments of greenish carbonatite, ≈(O3)	-3.4±0.01	14.6±0.1
18	T-205-23-3	Cement	-3.0±0.1	17.1±0.1
19	T-205-23-3	Fragments of variegated carbonatite	-3.1±0.1	16.2±0.1
20	T-205-23-3	Fragments of dolomitic carbonatite, (O1)	-3.8±0.1	12.8±0.3
21	T-205-23-3	Fragments of greenish carbonatite	-3.1±0.1	15.9±0.1
22	TM-442	Limestone of the Ulakhan-Kurung Formation (R_1uk)	0.12 0.89	21.85 23.54
23	G-2A/86 [1]	Marbled carbonate rocks of Tomtor complex exocontact	-3.4 -2.1	20.8 22.4
24	G-2Б/86 [1]		-2.1 -2.0	23.3 23.0
25	Mean (No 22-24)		-1.43	22.48
26	1076/2 [2]	Carbonate rocks (dolomites) of the Kotuikan Formation (R1kt) of the Billyakh series of the Anabar uplift	-2.7 -3	25.3 25.1
27	1093/1 [2]		-0.4	25.9
28	1094/2 [2]		-1.4	25.5
29	3075/1 [2]		-0.5	25.6
30	3075/2 [2]		-0.5 -0.6	26.2 26.0
31	3075/5[2]		-0.7	24.8
32	Mean (No 26-31)		-1.23	25.55

Note: No. 1-21 corresponds to the number shown in Figure 3. [1] – [Pokrovsky et al., 1990]; [2] – [Gorokhov et al., 2019]